the source term given by Eq. (10c) simplifies to

$$S(\phi,\psi) \cong -2e^{i\gamma}\{i(k_t A_t^*/\beta_\infty^2 - k_n A_n \beta_\infty)\Omega$$

$$-i(k_n A_t^* + k_t A_n/\beta_\infty)\theta$$

$$+(A_t^* M_\infty^2/\beta_\infty^2)\Omega' - (A_n M_\infty^2/\beta_\infty)\theta'\} \quad (14b)$$

where terms of $0(\epsilon^2)$ have been neglected.

It is also useful to note that $T(w)$ is related to the complex velocity potential for an incompressible flow which is a transformation of the mean flow past the body of interest. The perturbation velocity potential for the linearized compressible mean flow satisfies $\beta_\infty^2 \partial^2\Phi/\partial x^2 + \partial^2\Phi/\partial y^2 = 0$ and appropriate conditions on the body surface. Here (x,y) are Cartesian coordinates aligned with the uniform flow at infinity. Expanding the flow speed and angle in terms of the perturbation velocities we find to linear order

$$\partial\Phi/\partial x = -U_\infty \Omega/\beta_\infty \quad \partial\Phi/\partial y = U_\infty \theta \quad (15a,b)$$

We now introduce the coordinate transformation

$$\Phi'(x',y') = \Phi(x,y) \quad x' = x, y' = \beta_\infty y$$

The function Φ' then satisfies Laplace's equation and is the real part of an analytic function $F(z') = \Phi'(x',y') + i\Psi'(x',y')$ of $z' = x' + iy'$. $F(z')$ is determined by using the transformed boundary conditions on the body and $dF/dz' \to 0$ as $z' \to \infty$. Applying the coordinate transformation to Eqs. (15) and noting that $w = U_\infty z' + 0(\epsilon)$, we find

$$T(w) \cong -\beta_\infty F(w/U_\infty) + \text{const} \quad (16)$$

where terms of $0(\epsilon^2)$ have been neglected. The constant in Eq. (16) is determined by applying Eq. (13b).

In summary, we have shown that the equations governing disturbances to a subsonic compressible flow can be simplified significantly by using the tangent gas approximation for the mean flow. The transformed equations show that, for $(k_t^2 M_\infty^2/\beta_\infty^2 - k_z^2) > 0$, the irrotational portion of the disturbance will exhibit propagating wave behavior throughout the flowfield. When the mean flow perturbation is small, the equations can be further simplified. All quantities in the equations are then given explicitly in terms of a complex velocity potential and its derivatives. The complex velocity potential can be determined by a simple transformation of the equation for the linearized compressible mean flow past the body of interest.

Acknowledgment

The work described herein was financially supported by the General Electric Company Aircraft Engine Business Group under the Independent Research and Development Program.

References

[1] Hunt, J.C.R., "A Theory of Turbulent Flow Round Two-Dimensional Bluff Bodies," *Journal of Fluid Mechanics*, Vol. 61, 1973, pp. 625-706.

[2] Goldstein, M. E., "Unsteady Vortical and Entropic Distortions of Potential Flows Round Arbitrary Obstacles," *Journal of Fluid Mechanics*, Vol. 89, 1978, pp. 433-468.

[3] Woods, L. C., *The Theory of Subsonic Plane Flow*, Cambridge University Press, London, 1961.

[4] Lighthill, M. J., "Drift," *Journal of Fluid Mechanics*, Vol. 1, 1956, pp. 31-53.

AIAA 81-4278

Forebody Drag Reduction

B. N. Pamadi*
Indian Institute of Technology, Bombay, India

I. Introduction

A BLUNT body traveling at high speeds through the atmosphere experiences aerodynamic heating. One of the ways to alleviate this effect is to eject a cool gas jet directed against the air stream from the nose of the body.[1-3] The ejected gas flows back over the nose of the body and forms a protecting blanket of low temperature fluid. When the momentum of the jet efflux exceeds a certain critical value, the bow shock wave bulges out and stands away from the body surface and takes a form appropriate to a new body consisting of the original body with a protrusion due to jet flow (Fig. 1). The boundary of this protrusion is called the interface, the stream surface between the jet flow and the main stream flow. A conical, "dead air region" is formed around the jet and in the vicinity of the nose. The pressure on the body within the dead-air region is greatly reduced compared with pressures for no ejection (Fig. 1b). Thus, in addition to heat flux reductions, the forebody pressure drag also decreases considerably. Warren[1] considered this problem mainly with the objective of finding ejection conditions for achieving optimum heat flux reductions. Romeo and Sterret[2] studied the effect of a blowing gas jet on the form and location of bow shock wave. Finley[3] concerned himself mainly with the task of semiempirical prediction of the flow model. Both Warren[1] and Finley[3] have reported several pressure measurements over the forebody. However, full note of the large reductions in the forebody pressure drag has not been taken by these authors. It also appears that this point has not received further attention in literature.

In this Note the forebody pressure distributions taken from the studies of Warren[1] and Finley[3] have been integrated to deduce the corresponding drag coefficients. From this exercise, it is observed that significant forebody drag reductions can be achieved by this technique. Further, it is also shown that these data can be effectively correlated using a momentum coefficient which characterizes the jet efflux and freestream conditions.

II. Description of the Flow Pattern

We introduce a momentum coefficient to characterize the jet efflux

$$C_F = \left[p_j \frac{\pi}{4} d_j^2 + w_j v_j\right] \Big/ \left[\frac{1}{2}\rho_\infty V_\infty^2 \frac{\pi}{4} d_m^2\right] \quad (1)$$

where p_j is the static pressure at jet exit, v_j the jet exit velocity, w_j the jet mass flow rate, and V_∞ the freestream velocity.

For small values of momentum of the jet efflux ($C_F \leq 0.015$), no noticeable change occurs in the basic flow pattern, which comprises of a strong bow shock wave standing close to the body. When C_F exceeds 0.015, the bow shock wave begins to bulge out. Except for a small range of total pressures of the jet when the flow pattern is unsteady, the

Received Oct. 16, 1980; revision received May 1, 1981.

*Assistant Professor, Dept. of Aeronautical Engineering; presently, NRC-NASA Associate, NASA Langley Research Center, Hampton, Va..

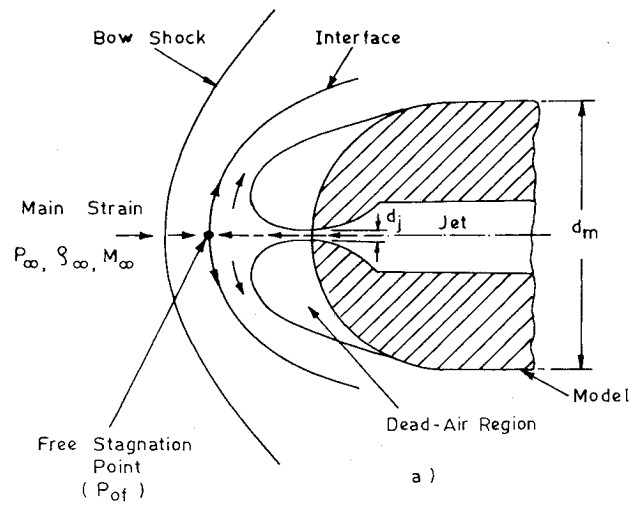

Fig. 1 Basic features of the flow.

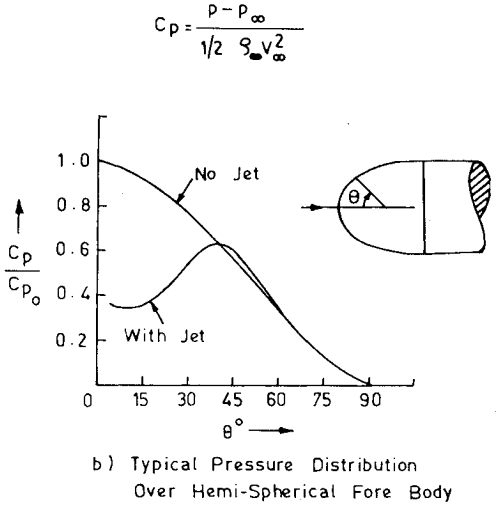

b) Typical Pressure Distribution Over Hemi-Spherical Fore Body

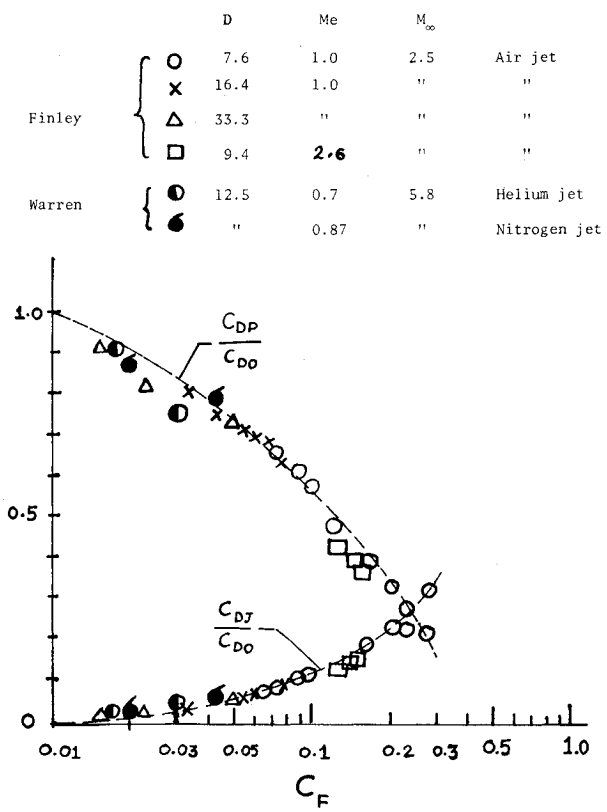

Fig. 2 Variation of C_{D_p} and C_{D_j} with C_F.

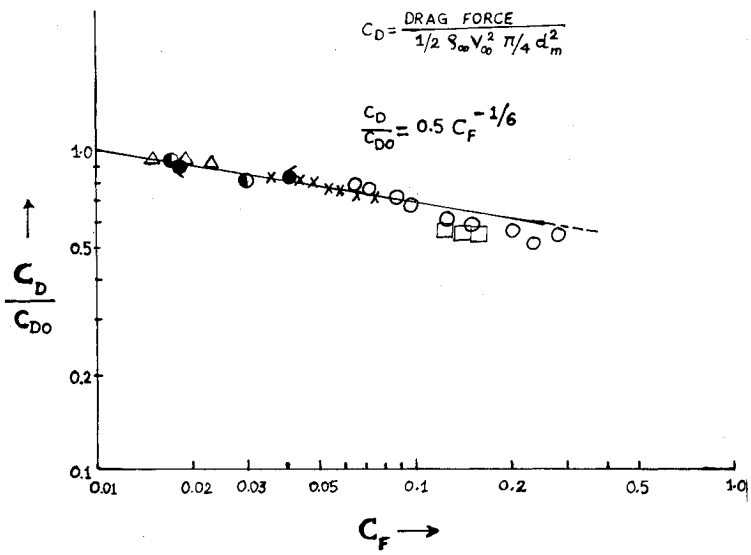

Fig. 3 Correlation of forebody drag reductions.

main flow separates ahead of the model, thereby leaving a roughly conical "dead-air region" in the vicinity of the nose. The characteristics of the pressure distribution are shown in Fig. 1b.

III. Results and Discussion

The forebody drag coefficients obtained from surface pressure integration and taking into account the drag caused by upstream facing jet are presented in Figs. 2 and 3. Here the skin friction drag is ignored because it is negligible compared to pressure drag. Further, it is assumed that the base pressure p_b is equal to freestream static pressure p_∞.

Finley's[3] model consisted of a hemispherical nose fitted to the cylindrical aft body. He used air jets issuing out of converging nozzles at exit Mach numbers M_e of 1.0 and 2.6. However, the majority of measurements were carried out at $M_e = 1.0$. The parameter D, which is the ratio of model diameter d_m to jet diameter d_j varied from 7.6 to 33.3. The freestream Mach number M_∞ was always equal to 2.5. The forebody in Warren's experiments[1] consisted of a portion of a cone of 10-deg semiangle with apex rounded with a spherical segment. The freestream Mach number was equal to 5.8. He employed helium and nitrogen gas jets for ejection. The jet exit Mach number was in the range 0.7-0.87. The parameter D was equal to 12.5.

The basic drag coefficients (C_{D_0}), are: a) Finley's model ($M_\infty = 2.5$), $C_{D_0} = 0.87$; b) Warren's model ($M_\infty = 5.8$), $C_{D_0} = 0.81$. These values compare favorably with those given by Hoerner,[4] which are, respectively, equal to 0.86 and 0.90. In view of this difference in basic drag coefficients, the normalized drag coefficients are plotted in Figs. 2 and 3.

The gas jet issuing against freestream adds to the drag, thus offsetting the drag reduction due to fall in the static pressures in the "dead-air region." This component of the drag coefficient (C_{D_j}) is given by the following expression

$$C_{D_j} = \left[(p_j - p_b)\frac{\pi}{4}d_j^2 + w_j v_j\right] \Big/ \left[\frac{\rho}{2} V_\infty^2 \frac{\pi}{4} d_m^2\right] \qquad (2)$$

As stated earlier, $p_b = p_\infty$ is assumed.

From Fig. 2 we observe that C_{D_j} rises sharply with an increase in jet momentum, and at $C_F = 0.23$ becomes equal to the drag coefficient resulting from pressure distribution (C_{D_p}). Beyond this point C_{D_j} is higher than C_{D_p}. Unfortunately, enough experimental data are not available for larger values of C_F. However, from the only available data at $C_F = 0.25$ (Fig. 3), we observe that the forebody drag coefficient at this value of C_F is higher than that at $C_F = 0.23$. Thus for any further increase in C_F, the trend will reverse and the forebody drag coefficient starts increasing. Therefore it can be inferred that the maximum achievable forebody drag reduction using this technique is limited to 50% by employing C_F around 0.23-0.25.

From Fig. 3 we note that the forebody drag coefficients deduced from Warren[1] and Finley's[3] experimental data correlate well in terms of a single parameter C_F. The deviation observed at higher values of C_F is apparently caused by the reversal of trend mentioned earlier. The correlation can be expressed mathematically as

$$C_D = \tfrac{1}{2} C_{D_0} C_F^{-1/6}, \quad 0.015 < C_F < 0.25 \tag{3}$$

The forebody drag reduction due to upstream facing jet is very similar to that of a protruding solid spike from the leading edge of a blunt body. The problem of a blunt body with leading edge spike at high speeds has been studied by a number of investigators, and their work has been discussed in detail by Chang.[5] A thin protruding probe, called a spike, mounted in front of a blunt body moving at high speeds is capable of reducing the forebody drag due to flow separation on the probe. The flow separation occurs because the boundary layer on the probe interacts with the shock wave generated at the junction with the body. In front of the body and between the oblique shock wave and the probe, a conical region of separated flow is formed in which the pressure is greatly reduced, as in the present problem. From the results presented by Chang,[5] it is seen that a forebody drag reduction of up to 50% can be achieved. The forebody drag coefficient of a spiked body is not very sensitive to Mach or Reynolds number.

In summary, we observe that the mechanisms of forebody drag reduction either by a spike or by a forward facing jet are quite similar. The maximum drag reductions achievable are also of the same order. However, a forward facing jet has the additional capability of reducing aerodynamic heating, which can be quite severe at high Mach numbers. Using the correlation presented in this work, the ejection parameters can be chosen to achieve maximum permissible forebody drag reduction by the technique suggested here.

References

[1] Warren, C.H.E., "An Experimental Investigation of the Effect of Ejecting a Coolant Gas at the Nose of a Bluff Body," *Journal of Fluid Mechanics*, Vol. 8, 1960, pp. 400-417.

[2] Romeo, D. J. and Sterret, D. R., "Exploratory Investigation of the Effect of a Forward-Facing Jet on the Bow Shock of a Blunt Body in a Mach Number 6 Free Stream," NASA TN D-1605, Feb. 1963.

[3] Finley, P. J., "The Flow of a Jet From a Body Opposing a Supersonic Free Stream," *Journal of Fluid Mechanics*, Vol. 26, Pt. 2, 1966, pp. 337-368.

[4] Hoerner, S. F., *Fluid Dynamic Drag*, Published by the author, 1965, pp. 18-13 to 18-24.

[5] Chang, P. K., "Separation of Flow," *International Series of Monographs in Interdisciplinary and Advanced Topics in Science and Engineering*, Vol. 3, Pergamon Press, New York, 1970, pp. 452-530.

AIAA 81-4279

Potential of Transformation Methods in Optimal Design

Ashok D. Belegundu* and Jasbir S. Arora†
The University of Iowa, Iowa City, Iowa

I. Introduction

THE purpose of this Note is to present a general framework for the efficient use of transformation methods in optimal design of large structural and mechanical systems. The term "transformation method" is used to describe any method that solves the constrained optimization problem by transforming it into one or more unconstrained optimization problems.

A basic difficulty in optimal structural design is that the evaluation of constraint functions and their gradients is very expensive. This is because many constraints of the design problem are implicit functions of design variables. The transformation methods essentially collapse all constraints of the design problem into one equivalent constraint[1] which serves as a penalty term for the transformation methods. This is very desirable for structural design applications, since it implies that one has to calculate the derivative of only one implicit function as compared to the calculation of derivatives of several implicit functions in other methods. Therefore, transformation methods can result in substantial computational savings in optimal design of structural and mechanical systems.

There are three classes of transformation methods that have been discussed in the literature: the penalty function, the barrier function, and the multiplier (or augmented Lagrangian) methods. The penalty and barrier methods have been referred to as sequential unconstrained minimization techniques (SUMTs) by Fiacco and McCormick.[2] SUMTs possess a number of undesirable properties. The weaknesses are most serious when a controlling parameter r is large. For large r, the penalty and barrier functions are ill-behaved near the boundary of the constraint set where the optimum points usually lie. Furthermore, it is shown[3,4] that the Hessian matrix of the unconstrained function becomes ill-conditioned as $r \to \infty$. In spite of these difficulties, SUMTs have been successfully used for many structural and mechanical system design applications. Notable among this body of literature are the works of Schmit[5] and Haftka.[6] More references on works of these authors may be found in Refs. 5 and 6.

The multiplier methods have been developed in the recent literature to alleviate some of the numerical difficulties encountered in SUMTs. These methods do not require large values of the controlling parameters, and also possess better convergence properties than SUMTs.[7]

II. Optimal Design Problem and Computation of Derivatives

To present ideas of the transformation methods as they apply to the structural and mechanical system design, a simplified model of the design problem is considered. It is understood that the methods presented here are applicable to more complex models for the design problem.[5,6,8]

The optimal design problem is defined as follows: minimize

$$\psi_0(b,z) \tag{1}$$

Received March 16, 1981.

*Research Assistant, Division of Materials Engineering. College of Engineering.

†Professor, Division of Materials Engineering. College of Engineering.